View metadata, citation and similar papers at core.ac.uk

brought to you by CORE

provided by Loughborough University Institutional Repository

This item was submitted to Loughborough's Institutional Repository (https://dspace.lboro.ac.uk/) by the author and is made available under the following Creative Commons Licence conditions.

creative commons

COMMONS DEED

Attribution-NonCommercial-NoDerivs 2.5

You are free:

- to copy, distribute, display, and perform the work

Under the following conditions:

Attribution. You must attribute the work in the manner specified by the author or licensor.

Noncommercial. You may not use this work for commercial purposes.

No Derivative Works. You may not alter, transform, or build upon this work.

- For any reuse or distribution, you must make clear to others the license terms of this work.
- Any of these conditions can be waived if you get permission from the copyright holder.

Your fair use and other rights are in no way affected by the above.

This is a human-readable summary of the Legal Code (the full license).

Disclaimer

For the full text of this licence, please go to:
http://creativecommons.org/licenses/by-nc-nd/2.5/

Atmospheric-pressure gas breakdown from 2 to 100 MHz

J. L. Walsh, Y. T. Zhang, F. Iza, and M. G. Kong[a)]
Department of Electronic and Electrical Engineering, Loughborough University, Loughborough, Leicestershire LE11 3TU, United Kingdom

(Received 20 October 2008; accepted 18 November 2008; published online 5 December 2008)

We report a detailed study of breakdown voltage of atmospheric-pressure helium gas between two parallel-plate electrodes from 2 to 100 MHz. Experimental data show that the breakdown voltage reduces initially with increasing frequency due to a diminishing contribution of drift-dominated electron wall loss and then begins to increase with increasing frequency. The latter is contrary to the current understanding that relies largely on the electron wall loss mechanism. Particle-in-cell simulation suggests that rapid oscillation of the applied voltage prevents electrons from reaching their maximum achievable kinetic energy, thus compromising the ionization efficiency and increasing the breakdown voltage. © *2008 American Institute of Physics*.
[DOI: 10.1063/1.3043449]

Atmospheric pressure glow discharges (APGDs) have recently commanded much attention as an emerging subject area of considerable scientific depth and application potential.[1] In search of greater application efficacy, a major thrust of current APGD research is more efficient production of reactive plasma species while maintaining tight control of their notorious instabilities. With large electron density and low breakdown voltage, radio-frequency (rf) APGDs are attractive and have found many important applications typically at 13.56 MHz.[1] The expansion of their application impact has recently prompted interest of venturing into the very-high frequency (VHF) band of 30–300 MHz (Ref. 2) because of better plasma stability at high frequencies.[3] However, there are surprisingly few reports of breakdown of rf APGD, most of which are for frequencies below 50 MHz and modest reduced electric field of $E/N=(0.1-1.0)\times10^{-19}$ V m^2 in an inert gas (e.g., helium or argon).[4–7] For molecular gases, breakdown studies of VHF high-pressure plasmas are equally scarce[8,9] and often limited to atmospheric air with markedly higher reduced electric field of $E/N=(1.2-5.2)\times10^{-19}$ V m^2. These limited studies suggest that breakdown voltage decreases with increasing frequency due to a diminishing role of electron wall loss. More extensively studied is rf breakdown at low gas pressures, which is found to follow a similar frequency dependence.[10–12] However their pressure-gap product pd is usually well below 10 Torr cm whereas rf APGDs tend to have $pd>50$ Torr cm. These different parameter ranges make it difficult to reliably extrapolate the current understanding of rf APGD below 50 MHz and low-pressure VHF plasmas to atmospheric gas breakdown in the VHF band. In this letter, we report a combined experimental and simulation study of atmospheric helium breakdown from 2 to 100 MHz.

The experimental apparatus consisted of two parallel stainless-steel disks, each 4 cm in diameter and with a Rogowski profile. One electrode was connected to the rf power supply via a π-match network while the other was grounded. Helium gas was fed into the electrode housing unit at a rate of 5 slm (slm denotes standard liters per minute). To ensure reliable current and voltage measurements, a calibration procedure was employed to correct for phase and amplitude errors introduced due to parasitic impedances within the apparatus.[13] A computerized data acquisition system was employed to automatically record the rms current, rms voltage, and their phase angle at a regular interval. Experimentally, the breakdown voltage was determined first by identifying the point at which the differential impedance dV/di underwent a step change caused by the developing discharge. As an alternative, it was obtained at the point where the current-voltage phase angle reduced abruptly from 90°. The two methods were found to agree with each other within ±1 V. Nanosecond imaging was acquired using an Andor DH 720 iCCD camera. To quantitatively study electron production and loss under different breakdown conditions, a particle-in-cell (PIC) code was used based on the XPDP1 model with the model's own cross-section data[14] and using a large number of electrons (10^5-10^6).

Figure 1(a) shows breakdown characteristics at various electrode gaps of $d=0.5-2.0$ mm, corresponding to $pd=38-152$ Torr cm. The reduced electric field E/N was within into the $(4-13)\times10^{-21}$ V m^2 range. As an example of the breakdown event, plasma images immediately after gas breakdown are shown in Fig. 1(b) for the $d=2$ mm case at 2 MHz (no imaging was attempted at higher frequencies due to their very short rf cycle). Although streamers are com-

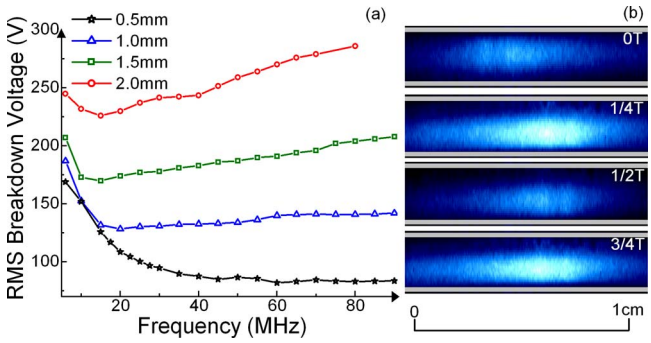

FIG. 1. (Color online) (a) Frequency dependence of breakdown voltage in various gap separations; (b) four 5 ns plasma images taken through one rf cycle at 2 MHz and $d=2$ mm. Grey regions in each image represent the two parallel electrodes.

[a)]Author to whom correspondence should be addressed. Electronic mail: m.g.kong@lboro.ac.uk.

 © 2008 American Institute of Physics

Downloaded 21 Aug 2009 to 158.125.80.71. Redistribution subject to AIP license or copyright; see http://apl.aip.org/apl/copyright.jsp

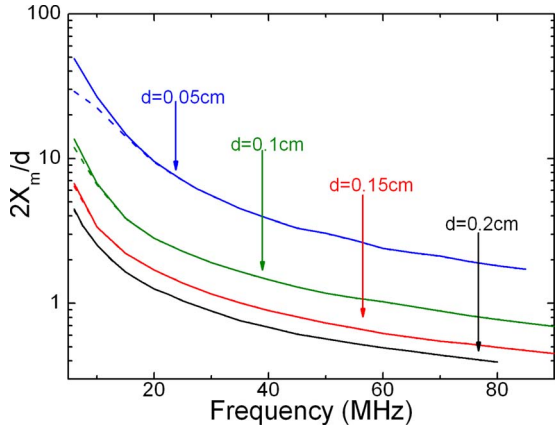

FIG. 2. (Color online) Normalized electron oscillation amplitude as a function of excitation frequency for $n_e=10^8$ cm^{-3} (solid curves) and $n_e=10^{12}$ cm^{-3} (dashed curves).

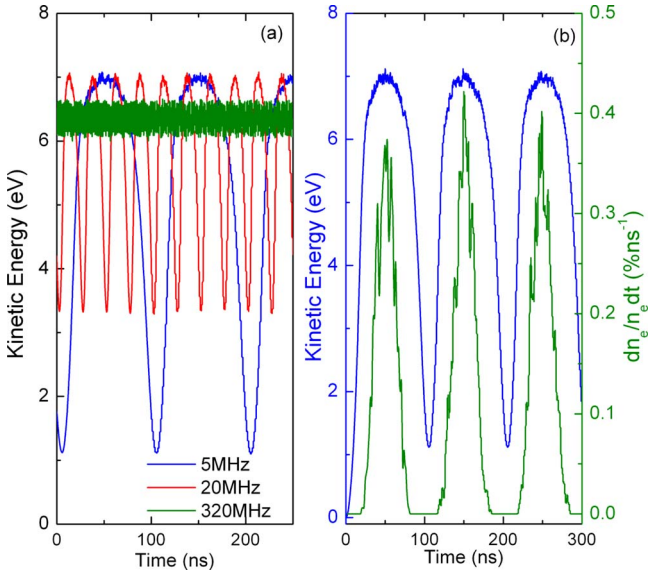

FIG. 3. (Color online) PIC simulation of the time evolution of (a) the particle-averaged electron kinetic energy at three different excitation frequencies at 100 V/mm; (b) the electron production rate and the particle-averaged electron kinetic energy at 5 MHz and 100 V/mm.

mon at large pd values,[15] no streamers were observed on a time scale of 5 ns [Fig. 1(b)] in our experiments ($pd=152$ Torr cm) and the discharge was spatially diffused. This suggests that VHF plasmas in our experiments did not result from a streamer-type breakdown.

Breakdown voltage V_b in Fig. 1(a) undergoes initially a rapid reduction with increasing frequency before its decrease slows down around 15–35 MHz depending on the electrode gap size. The frequency at which V_b starts to decrease is known as the second critical frequency.[9] The initial rapid reduction in breakdown voltage is similar to those observed for a helium rf APGD in the 1–30 MHz range[4] and for an argon rf APGD in the 1–50 MHz range,[6] as well as other rf breakdown studies.[8–12,16] It is due to a decreasing contribution of drift-dominated electron wall loss and may be explained by considering the electron oscillation in a high frequency field of $E_0 \cos \omega t$ with its oscillation amplitude given by[17]

$$x_m = \frac{eE_0/m_e}{\sqrt{[\omega^2 - \omega_p^2(2x_m/d)]^2 + \omega^2 v_c^2}}, \tag{1}$$

where m_e is the electron mass, d is the electrode gap distance, $\omega_p=\sqrt{e^2 n_e/\varepsilon_0 m_e}$ is the plasma frequency with e and n_e being electron charge and electron density, and v_c is the electron-neutral collision frequency, respectively. At atmospheric pressure and in the VHF band, the ratio of the excitation frequency to the collision frequency $f/v_c=3\times10^{-3}-3\times10^{-5}\ll1$. When $2x_m/d\approx1$, most electrons are just able to reach the electrodes. As the discharge starts to build up during breakdown, the electron density is initially low ($\omega_p\ll\omega$). Therefore Eq. (1) can be reduced to $x_m\approx(eE_0/m_e)/\omega v_c$. With increasing frequency, the electron oscillation amplitude eventually becomes smaller than $d/2$. This suggests that more electrons are trapped in the electrode gap[18] thus reducing the drift-dominated electron loss to the electrodes. This decreases the breakdown voltage [Fig. 1(a)] and is consistent with the current understanding of rf breakdown at atmospheric pressure. To see this without the above approximation, numerical solution of Eq. (1) is shown in Fig. 2 for $n_e=10^8$ and 10^{12} cm^{-3}. It is clear that with increasing frequency the value of $2x_m/d$ decreases monotonically, and this trend is almost independent of electron density. This confirms that with increasing frequency, electrons are progressively prevented from reaching the electrodes and as such the breakdown voltage reduces. Continuous increase in frequency eventually brings the electron oscillation amplitude well within the electrode gap distance ($2x_m/d<1$) and as a result makes the drift-dominated electron wall loss negligible. With diminishing drift-dominated electron wall loss, the decrease in the breakdown voltage slows down. This is the case when $d=0.5$ mm and also when $d\geq1$ mm up to $f=20$ MHz in Fig. 1(a).

The monotonic decrease of $2x_m/d$ would suggest a monotonic decrease in the breakdown voltage if rf breakdown depended on electron wall loss only. Above 20 MHz in Fig. 1(a), the increase in breakdown voltage with increasing frequency for $d=1.0$, 1.5, and 2.0 mm has not been reported for rf APGD[4–6] and low-pressure rf plasmas.[10–12,16] Following the same notation as that for the second critical frequency, we refer the frequency of the minimum breakdown voltage as the third critical frequency. Its underpinning physics cannot be explained by electron wall loss mechanisms and may relate to electron kinetic effects. For example, it is possible that with the excitation frequency being increased continually, the time available for electron acceleration before the polarity change in the applied voltage becomes increasingly limited. This may compromise effective electron heating and subsequent gas ionization by such inadequately accelerated electrons. In other words, the increase in breakdown voltage after $f=20$ MHz and for $d\geq1$ mm may be due to compromised electron heating at very high frequencies even though electron-wall loss may be minimized.

Equation (1) is ineffective in assessing the effect of electron heating as it does not contain electron kinetic information. To this end, PIC simulation was employed with electrons initially loaded at room temperature and then the motion of each electron was tracked in time as they underwent collisions with the background gas. The electrons were assumed to be in an infinitely large gap so that no wall losses took place, and their density was low enough not to perturb the applied field. Figure 3(a) shows that it is more difficult

Downloaded 21 Aug 2009 to 158.125.80.71. Redistribution subject to AIP license or copyright; see http://apl.aip.org/apl/copyright.jsp

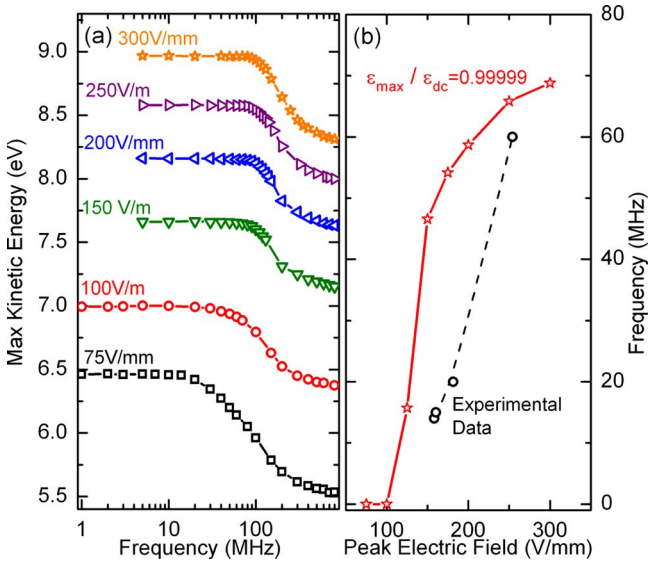

FIG. 4. (Color online) (a) Frequency dependence of the maximum particle-averaged electron kinetic energy acquired at different rf fields and (b) field dependence of the third critical frequency (dashed black line) and the PIC simulated corner frequency at which ε_{max} drops to 99.999% of ε_{dc}.

for electrons to reach their maximum kinetic energy at high frequencies. In the case of 5 MHz, Fig. 3(b) suggests that the particle-averaged electron kinetic energy ε_k is significantly rf-modulated, and its modulation is dynamically correlated with that of the net electron production rate dn_e/dt. This correlation suggests that the maximum electron kinetic energy ε_{max} at a given rf field may be used to represent the most efficient electron production and hence gas breakdown. Rapid time modulation of ε_k means that electrons may not be able to reach their theoretical maximum ε_{dc}, which is obtained when electrons are allowed to accelerate as long as possible without the effect of polarization change in the applied voltage, in other words, when the applied voltage is dc.

Figure 4(a) shows the maximum particle-averaged electron kinetic energy acquired in different driving rf fields as a function of frequency from 1 MHz to 1 GHz. Below 5 MHz, ε_{max} changes little for most rf electric fields considered and electrons can reach their theoretical maximum kinetic energy, i.e., $\varepsilon_{max}=\varepsilon_{dc}$. With increasing frequency at any given rf field, it is increasingly difficult for electrons to reach their theoretical maximum because they are deprived of adequate time for sufficient acceleration within each rf half cycle. At any given frequency, the electron kinetic energy can be increased closer to ε_{dc} by using larger rf fields, as shown in Fig. 4(a). At 40 MHz, the maximum particle-averaged electron kinetic energy is 6.3 eV at 75 V/mm and 8.9 eV at 300 V/mm. The former is about 3% below ε_{dc} at 75 V/mm whereas the latter is vertically ε_{dc} at 300 V/mm. General trends in Fig. 4(a) are consistent to the frequency dependence of the breakdown voltage in Fig. 1(a). For example, ε_{max} starts to decrease markedly near 20 MHz for 100 V/mm in Fig. 4(a), corresponding well to the two cases of $d=2.0$ and 1.5 mm in Fig. 1 where the minimum breakdown field of $E_0=\sqrt{2}\ V_b/d=160$ V/mm occurs at the same third critical frequency of 15 MHz. The corner frequency at which ε_{max} starts to decrease should correspond to the third critical frequency at which the breakdown voltage reaches its minimum. To see this more clearly, the frequency at which the maximum electron kinetic energy drops from the dc value is plotted in Fig. 4(b) against the peak electric field using PIC data in Fig. 4(a), together with the third critical frequency obtained from experimental data in Fig. 1(a). It is clear that their trends are similar, both increasing with the rf field because compromised electron heating at high frequencies can be compensated by a large driving rf field. The agreement in their rf field dependence suggests that compromised electron heating is indeed important in causing the increase in breakdown voltage at high frequencies.

Although the present work is concerned with atmospheric helium, its results should apply to VHF breakdown of other gases at high gas pressures. The expansion of rf APGD into the VHF band opens up previously unavailable parametric regimes within which to tailor their basic characteristics (e.g., electron temperature and electron density) and their reaction chemistry.[2] This work suggests that their breakdown voltage may experience a marked increase and may impose limitation on the range of appropriate VHF power sources. However this restriction can be mitigated by reducing the electrode gap, not only allowing for a lower breakdown voltage but also for a larger electric field. In Fig. 1(a), the minimum electric field calculated from the minimum breakdown voltage is 160 V/mm at $d=2$ mm and 232 V/mm at $d=0.5$ mm, respectively. This suggests that microplasmas may benefit particularly from VHF excitation.[19]

[1] A. Schütze, J. Y. Jeong, S. E. Babayan, J. Park, G. S. Selwyn, and R. F. Hicks, IEEE Trans. Plasma Sci. **26**, 1685 (1998).
[2] J. L. Walsh, F. Iza, and M. G. Kong, Appl. Phys. Lett. (to be published).
[3] J. J. Shi and M. G. Kong, Appl. Phys. Lett. **87**, 201501 (2005).
[4] J. Park, I. Henins, H. W. Herrmann, and G. S. Selwyn, Appl. Phys. Lett. **89**, 15 (2001).
[5] S.-Z. Li, J. G. Kang, and H. S. Uhm, Phys. Plasmas **12**, 093504 (2005).
[6] C. Schrader, L. Baars-Hibbe, K.-H. Gericke, E. M. van Veldhuizen, N. Lucas, P. Sichler, and S. Butthenbach, Vacuum **80**, 1144 (2006).
[7] J. J. Shi and M. G. Kong, J. Appl. Phys. **97**, 023306 (2005).
[8] J. A. Pim, Proc IEE **96**, 117 (1949).
[9] M. Aints, A. Haljaste, K. Kudu, and V. Adamson, J. Phys. D **28**, 81 (1995).
[10] V. A. Lisovskiy and V. D. Yegorenkov, J. Phys. D **31**, 3349 (1998).
[11] H. B. Smith, C. Charles, and R. W. Boswell, Phys. Plasmas **10**, 875 (2003).
[12] M. Radmilovic-Radjenovic and J. K. Lee, Phys. Plasmas **12**, 063501 (2005).
[13] L. P. Bakker, G. M. W. Kroesen, and F. J. de Hoog, IEEE Trans. Plasma Sci. **27**, 759 (1999).
[14] J. P. Verboncoeur, M. V. Alves, V. Vahedi, and C. K. Birdsall, J. Comput. Phys. **104**, 321 (1993).
[15] L. B. Loeb and J. M. Meek, J. Appl. Phys. **11**, 438 (1940).
[16] S. C. Brown and A. D. MacDonald, Phys. Rev. **76**, 1629 (1949).
[17] Y. P. Raizer, M. N. Shneider, and N. A. Yatsenko, *Radio-frequency Capacitive Discharges* (CRC, London, 1995).
[18] D. W. Liu, J. J. Shi, and M. G. Kong, Appl. Phys. Lett. **90**, 041502 (2007).
[19] J. J. Shi and M. G. Kong, Phys. Rev. Lett. **96**, 105009 (2006).

Downloaded 21 Aug 2009 to 158.125.80.71. Redistribution subject to AIP license or copyright; see http://apl.aip.org/apl/copyright.jsp